

Supporting Information Appendix

Supplementary Materials and Methods

***Plasmodium falciparum* culture and transfection.** The 3D7 strain, obtained from the Walter and Eliza Hall Institute (Melbourne, Australia), and the NF54(pfs47)DiCre strain(1), obtained from Moritz Treeck at The Francis Crick Institute, of *P. falciparum* were maintained *in vitro* in human O+ erythrocytes at 4% hematocrit in RPMI-1640 (Sigma) supplemented with 25 mM HEPES 4-(2-hydroxyethyl)-1-piperazineethanesulfonic acid (EMD Biosciences), sodium bicarbonate (Sigma), 50 mg l⁻¹ hypoxanthine (Sigma), and 0.5% Albumax II (Invitrogen) (2).

3D7-Cas9 parasites: 3D7 parasites were transfected with pUF1-Cas9 plasmid DNA. 3D7-Cas9 parasites were selected with the PfDHODH inhibitor N-(3-chloro-4-methylphenyl)-5-methyl-2-(trifluoromethyl)[1,2,4]triazolo[1,5-a]pyrimidin-7-amine (MMV665874 or AD1) at 150 nM (3).

PfBLEB-smV5^{Tet} parasites: approximately 100 µg of homology-directed repair template plasmid was linearized by digestion and transfected into 3D7-Cas9. This plasmid also expressed the PfBLEB-targeting guide RNA. PfBLEB-smV5^{Tet} parasites were maintained on 500 nM ATc. One day post transfection, drug pressure was applied with 2.5 nM WR99210 (Jacobus Pharmaceuticals). Integration of the construct was confirmed by PCR amplifying genomic DNA with oligos oJDD1525/oJDD2933. Tet aptamer size was confirmed by amplifying the aptamer with oligos oJDD2239/oJDD44 and digesting the PCR fragment with PspOMI and KpnI. Illumina-based next-generation sequencing performed on this isolate additionally confirmed integration (fastq files deposited in NCBI Sequence Read Archive, PRJNA813841).

PfBLEB^{KO} parasites: 3D7 parasites were transfected with pJDD339 plasmid DNA that contains 498 bp of homology at the N-terminus of the PfBLEB gene, followed by an in-frame smV5 epitope tag, the 2A ribosomal skip peptide, and the ScDHODH selectable marker (4), along with the human dihydrofolate reductase selectable marker under the control of the *P. falciparum* calmodulin promoter in the plasmid.

Following transfection PfBLEB^{KO} parasites were selected following the protocol in (5) with the following modifications: parasites were first selected on 2.5 nM WR99210 (Jacobus Pharmaceutical Company), then on 150 nM AD1. Integration of the targeting construct for PfBLEB^{KO} was confirmed by PCR with oligos oJDD4756/oJDD4489. Illumina-based next-generation sequencing performed on this isolate additionally confirmed integration (fastq files deposited in NCBI Sequence Read Archive, PRJNA842015).

PfCINCH-smMyc / PfBLEB-smV5 double-tagged parasites: 100 µg of homology-directed repair template plasmid was linearized by digestion and transfected into PfBLEB-smV5^{Tet} parasites along with a separate plasmid containing the PfCINCH-targeting guide RNA. One day post transfection, drug pressure was applied with 2.5 µg/ml blasticidin (RPI).

PfBTP2-3xHA strain was generated as previously described (3).

PfBLEB-TurboID parasites (3D7 or NF54-based): The homology-directed repair template was PCR amplified and transfected into 3D7-Cas9 or NF54(pfs47)DiCre parasites, along with a separate plasmid containing the PfBLEB-targeting guide RNA. From the onset of transfection, parasites were cultured in biotin-free media. One day post transfection, drug pressure was applied with 5 nM WR99210 (Jacobus Pharmaceutical Company) for one week, then with 2.5 nM WR99210 for two additional weeks. Integration of the construct was confirmed by amplifying the genomic DNA using oligos oJDD56/oJDD6010.

3D7-PfBLEB-HaloTag/PfCINCH-mNeonGreen: 3D7 was transfected with pRR205 (PfCINCH-mNeonGreen targeting plasmid) and pRR99 (PfCINCH CRISPR guide) and selected with WR99210. This parasite strain was subsequently transfected with pAM99 (PfBLEB-HaloTag) and pRLC104 (PfBLEB CRISPR guide) and selected with blasticidin.

PF3D7_1435600-smV5 parasites: 100 µg of homology-directed repair template plasmid was linearized by digestion and transfected into 3D7-Cas9 parasites along with separate plasmids containing the PF3D7_1435600-targeting guide RNA. One day post transfection, drug pressure was applied with 2.5

nM WR99210 (Jacobus Pharmaceuticals). Integration of the construct was confirmed by PCR amplifying genomic DNA with oligos oJDD6917/oJDD2933.

Individual transgenic clones for PfBLEB-smV5^{Tet} and PfBLEB^{KO} parasite lines were obtained by limiting dilution. All sequences for oligonucleotides are provided in *SI Appendix*, Table S3.

Experimental animals. Six- to eight-week old Swiss Webster female mice from Envigo were used for all experiments performed with *Plasmodium yoelii* 17XNL strain parasites. All protocols with mice were approved by the Pennsylvania State University Institutional Animal Care and Use Committee (IACUC protocol # 42678) and experiments conformed to the Association for Assessment and Accreditation of Laboratory Animal Care (AAALAC) guidelines.

Reverse Genetics of *P. yoelii* 17XNL Parasites. Conventional gene editing approaches for *P. yoelii* were used to append a C-terminal GFP tag to PyBLEB as described previously (6). Mouse blood infected with *Plasmodium yoelii* (17XNL strain) was collected via cardiac puncture, placed into 5ml complete RPMI (cRPMI; 20% v/v FBS in RPMI 1640 with gentamicin (50mg/ml)), and pelleted at 200 x g for 8 minutes (no brake). Serum and cRPMI were removed and cells were resuspended in 30ml cRPMI per mouse equivalent into a sealed T75 flask gassed with 5% CO₂, 10% O₂, and 85% N₂. Parasites were cultured for 14 hours at 37°C while shaking (50-60rpm) and were confirmed to have been synchronized to mature parasites via smear and Giemsa staining. After verification, 10ml 26.7% w/v Accudenz dissolved in 5mM Tris pH 7.5 (at RT), 3mM KCl, and 0.3mM EDTA in 1x PBS without calcium and magnesium was layered underneath 30ml of parasite culture in a 50 ml conical tube. The mixture was spun at 200 xg for 20 minutes with no brake, and schizonts that migrated to the interface of the two layers were collected. Schizonts were pelleted by centrifugation at 200 xg for 10 min with no brake, and then resuspended in 50-200µl of cRPMI. Ten to fifteen micrograms of 1mg/ml linearized

plasmid in ddH₂O was added to 100ul of cytomix (120mM KCl, 0.15mM CaCl₂, 2 mM EDTA, 5 mM MgCl₂, 8.66mM K₂HPO₄ pH 7.6 (at RT), 1.34 mM KH₂PO₄ pH 7.6 (at RT), and 25mM HEPES pH 7.6 (at RT)). Ten microliters of purified schizonts were added to the DNA containing cytomix and mixed with a wide-bore pipette before getting transferred to a cuvette. Electroporation was done using an Amaxa Nucleofector 2b with program T-016 and was immediately followed by the addition of 50µl of cRPMI prior to injecting intravenously into mice. The recipient mice were placed on pyrimethamine (0.007% w/v final concentration, Fisher Scientific, Cat# ICN19418025) administered in the drinking water, one day post transfection and remained on drug for three days before replacing with regular water. Parasites were allowed to reach a parasitemia of 1%. Infected blood (100µl) was used to infect a naïve mouse by intraperitoneal (IP) injection and the drug cycling was repeated. Upon reaching 1% parasitemia, the mouse was exsanguinated, using a portion of the infected blood to store in cryovials in liquid nitrogen. The remainder of the infected blood was used to extract genomic DNA for genotyping PCR. Upon confirming a mixed population of transgenic and wild type parasites for PyBLEB-GFP, frozen cryovials were used to infect mice via IP injection and parasites were used for microscopy analysis.

Plasmid construction.

pJDD342 (PfBLEB-smV5^{Tet}): 5' and 3' homology regions (HRs) were PCR amplified from 3D7 genomic DNA using primers oJDD4162/oJDD4165 and oJDD4161/oJDD4163. PCR Sequence Overlap Extension (PCR SOE) was used to combine 5' HR, 3' HR, and codon altered gene block (IDT DNA) using oJDD4161/oJDD4401. The product was cut with NotI/NcoI and ligated into pRR93 to create pRLC79. The U6 guide cassette was generated by PCR SOE using oJDD4564/oJDD4571/oJDD4572/oJDD3059, digested with PstI/AvrII, and ligated into pRLC79 to create pJDD342.

pJDD339 (PfBLEB^{KO}): smV5-2A was PCR amplified from pJR207 with oJDD3273/oJDD4546, and

yURA1 was PCR amplified from pSAB85 with oJDD4547/oJDD4548. The products were fused by PCR SOE with oJDD3273/oJDD4548, digested with NotI/MluI, and ligated into pJR207 to create pJDD333. The 5' end of PfBLEB was PCR amplified from 3D7 genomic DNA using oJDD4159/oJDD4160, digested with NotI/MluI, and ligated into pJDD333 to create pJDD339.

pSL1528 (PyBLEB-GFP): 3' HR and 3' Open Reading Frame (ORF) were PCR amplified from Py17XNL genomic DNA using primers oSL28-59/oSL28-60 (3' HR) and oSL28-63/28-64 (ORF). PCR SOE of ORF and 3' HR was done with oSL28-59/oSL28-64. PCR SOE was ligated into the StuI site of pCR-Blunt (Thermo Fisher) to create pSL1526. PCR SOE sequence was verified in pSL1526 using Sanger Sequencing at the PSU Genomics Core. PCR SOE insert from pSL1526 was digested with KpnI/SpeI and ligated into similarly digested vector pSL0442 to create pSL1528.

pBNA03 (PfBLEB-TurboID): The PfBLEB homology-directed repair template sections from pJDD342 were excised using NotI/NcoI and ligated into pAM11.

pRLC104 (PfBLEB-targeting guide RNA): oJDD5238 and oJDD5239 were annealed, phosphorylated, and ligated into BpiI-digested pRR216.

pAM131(PF3D7_1435600-smV5): 5' and 3' HRs were PCR amplified from 3D7 gDNA using oJDD6449/6450 and oJDD6447/6448. PCR SOE was used to combine the 5' HR, 3' HR, and codon altered gene block (IDT DNA) using oJDD6575/oJDD6576. This product was cut with NotI/NcoI and ligated into plasmid pPG03 to create pAM131.

pAM148, 151, and 152 (PF3D7_1435600-targeting guide RNA): oJDD6453/oJDD6454, oJDD6577/oJDD6578, or oJDD6579/oJDD6580 were annealed, phosphorylated, and ligated into BpiI-digested pRR216.

pAM99 (PfBLEB-HaloTag): HaloTag was digested from pRR223 with NcoI/KpnI and ligated into pBNA01.

REFERENCES for Supplementary Materials and Methods.

1. M. Tiburcio *et al.*, A Novel Tool for the Generation of Conditional Knockouts To Study Gene Function across the Plasmodium falciparum Life Cycle. *mBio* **10** (2019).
2. W. Trager, J. B. Jensen, Human malaria parasites in continuous culture. *Science* **193**, 673-675 (1976).
3. R. M. Rudlaff, S. Kraemer, V. A. Streva, J. D. Dvorin, An essential contractile ring protein controls cell division in Plasmodium falciparum. *Nat Commun* **10**, 2181 (2019).
4. S. M. Ganesan *et al.*, Yeast dihydroorotate dehydrogenase as a new selectable marker for Plasmodium falciparum transfection. *Mol Biochem Parasitol* **177**, 29-34 (2011).
5. J. Birnbaum *et al.*, A genetic system to study Plasmodium falciparum protein function. *Nat Methods* **14**, 450-456 (2017).
6. L. M. Bowman, L. E. Finger, K. J. Hart, S. E. Lindner, Definition of constitutive and stage-enriched promoters in the rodent malaria parasite, Plasmodium yoelii. *Malar J* **19**, 424 (2020).

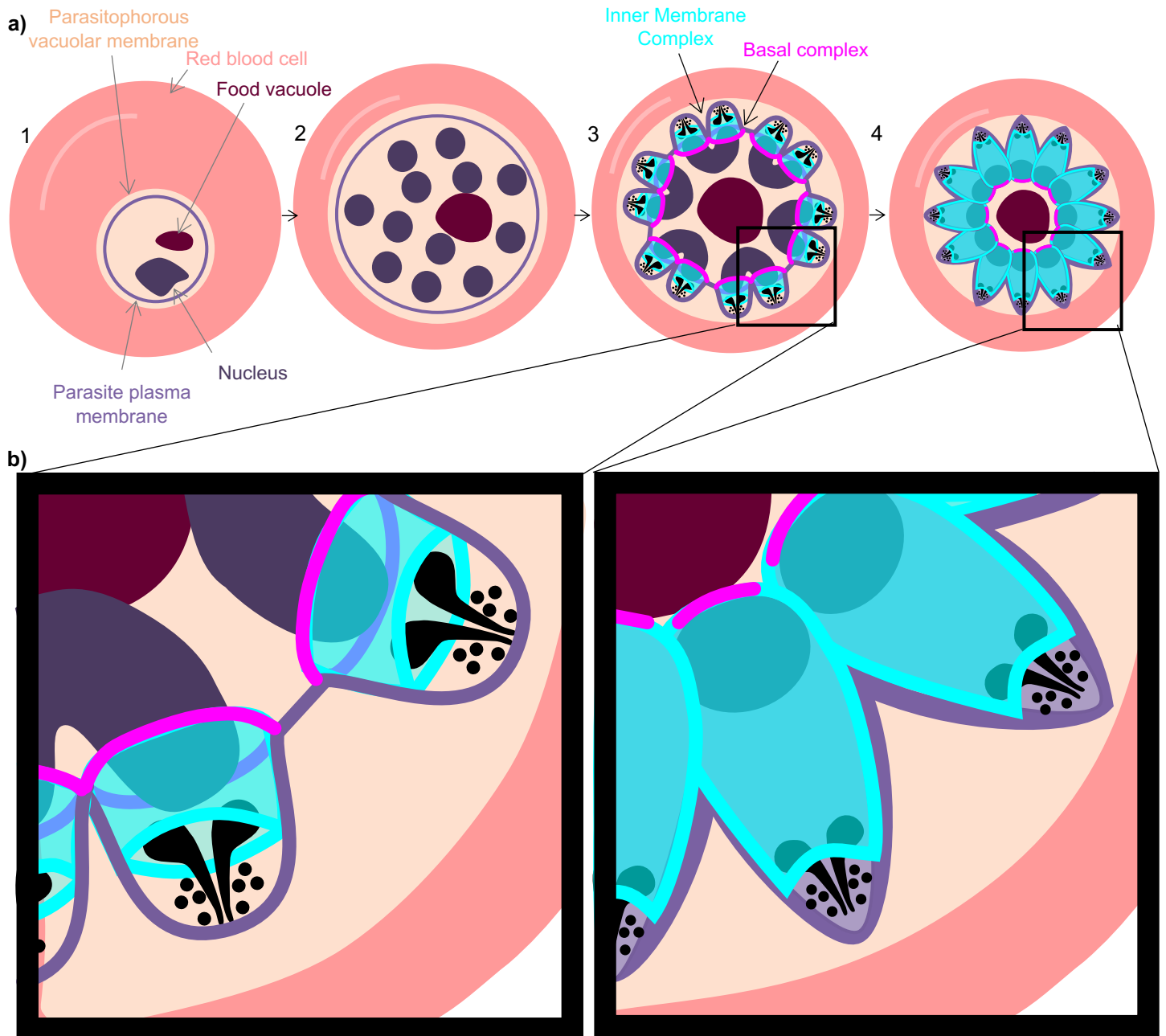


Fig. S1. The basal complex and inner membrane complex play a role in schizogony.

a) *Plasmodium falciparum* replicates asexually in red blood cells during schizogony: (1) A trophozoite inside a red blood cell. (2) The parasite replicates its DNA and organelles asynchronously. (3) A final semi-synchronized round of DNA replication occurs and daughter merozoites bud off from the mother cell membrane. (4) Replication and segmentation complete, producing 16-32 daughter merozoites. **b)** The inner membrane complex (cyan) contributes to segmentation of each daughter cell and segregation of organelles. The basal complex (magenta) is on the leading edge of the inner membrane complex.

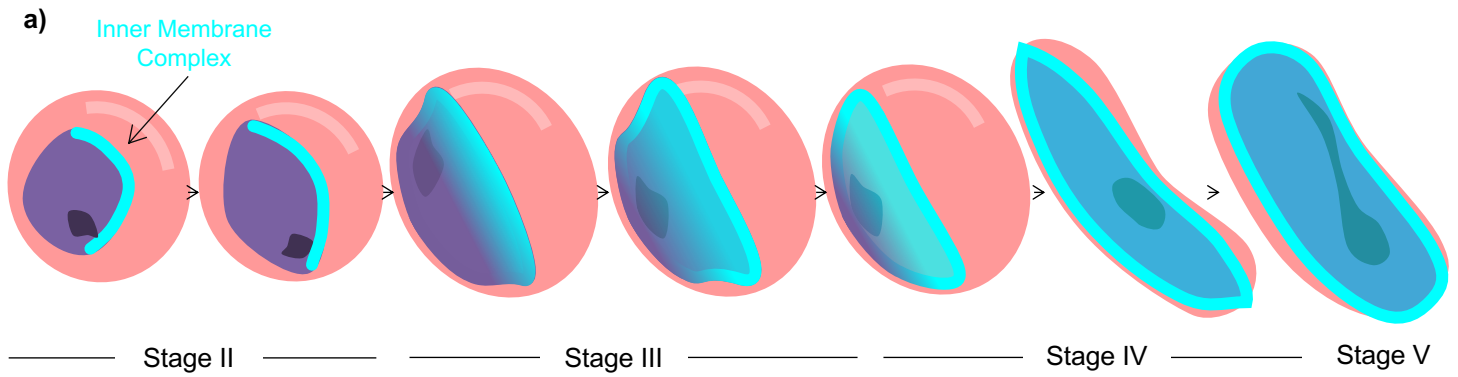
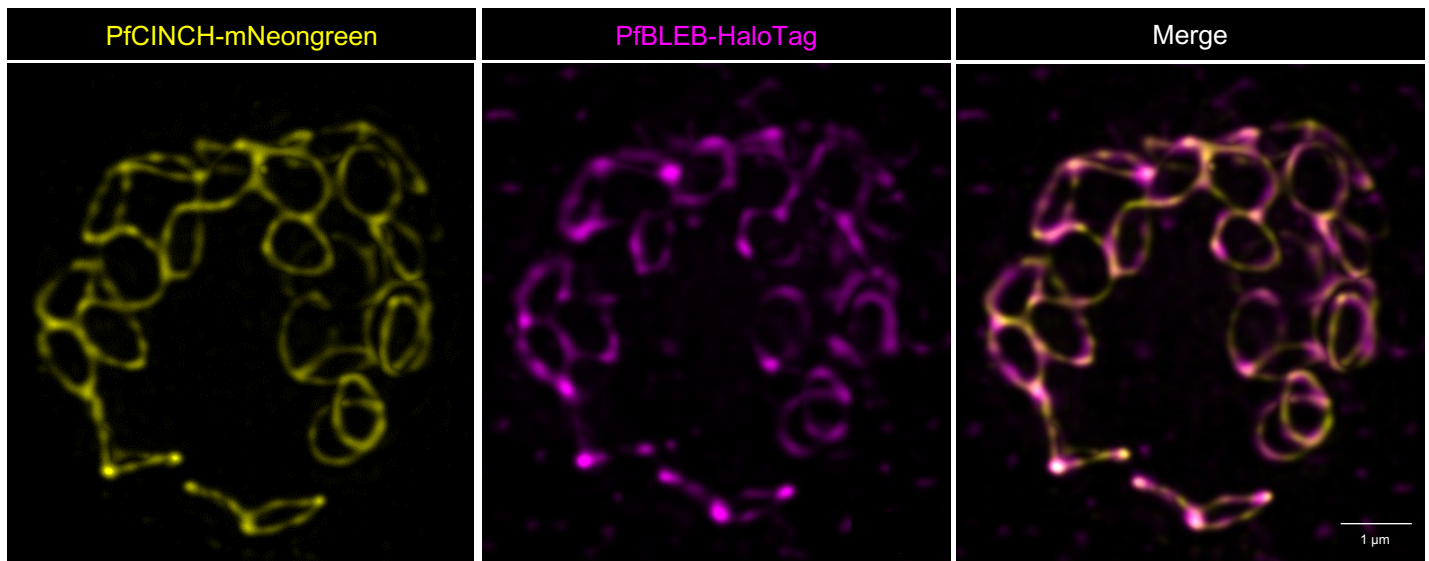


Fig. S2. The inner membrane complex plays a role in gametocytogenesis.

Plasmodium falciparum develops into transmission-stage parasites through the multi-staged process of gametocytogenesis. The inner membrane complex (cyan) serves as a structural support as gametocytes mature. Initially, the inner membrane complex lines one edge of the gametocyte but expands to envelop the gametocyte as it matures.

a)



b)

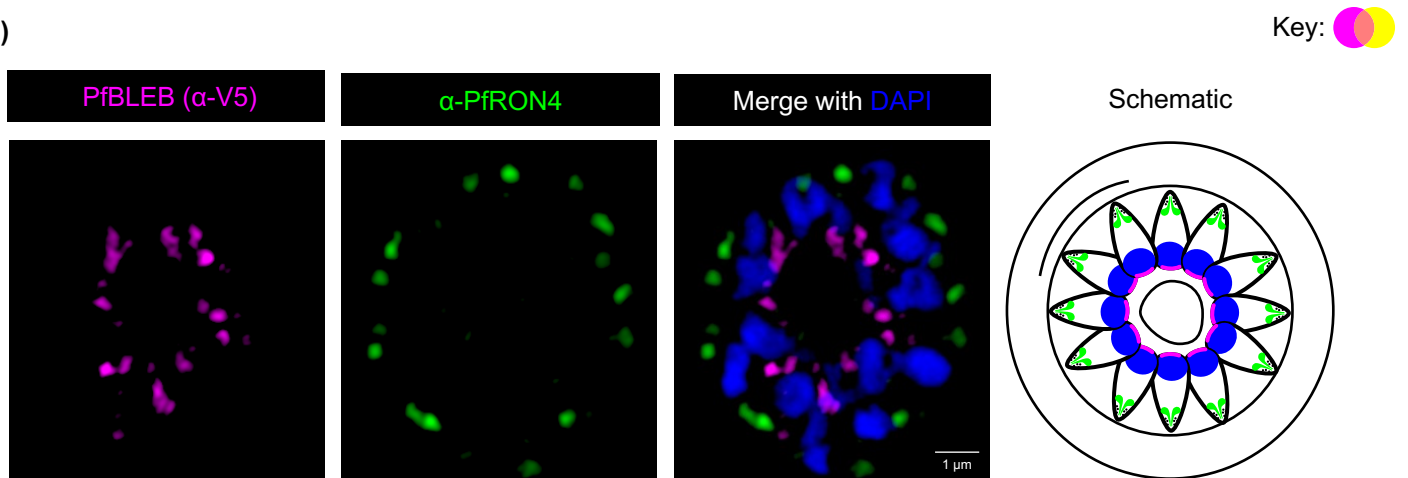


Fig. S3. PfBLEB localizes to the basal complex. a) Immunofluorescence demonstrates localization of PfBLEB-HaloTag (magenta) and PfCINCH-mNeonGreen (yellow) to the basal complex during segmentation in live cells. Maximum intensity projections of SIM² images. See Supplemental Movie 1. Scale bar = 1 μm . b) Immunofluorescence of PfBLEB-smV5^{Tet} shows separation of PfBLEB (magenta) and apical marker, PfRON4 (green), at the end of segmentation. Single Z-slice of SR-SIM images. Scale bar = 1 μm .

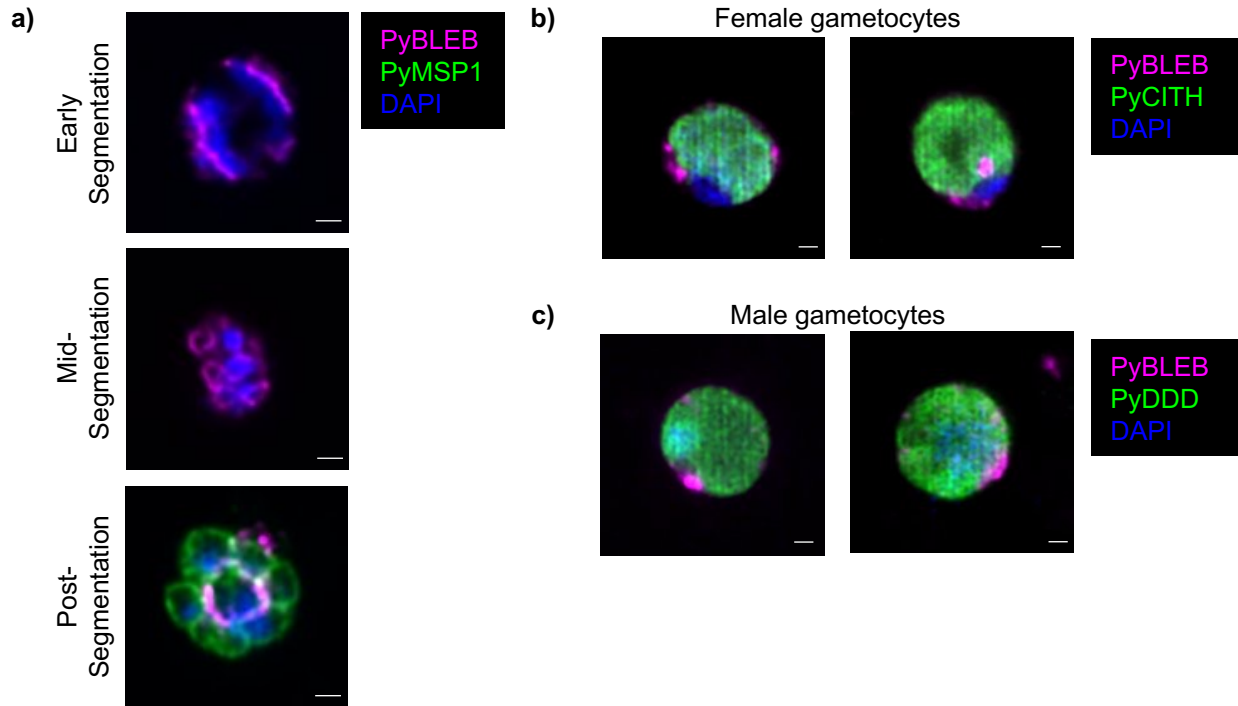


Fig. S4. *Plasmodium yoelii* BLEB is expressed in asexual and gametocyte stages. **a)** Immunofluorescence microscopy of *Plasmodium yoelii* BLEB (magenta) demonstrates dynamic localization similar to the basal complex in schizont stage parasites. In fully segmented schizonts (bottom panel), MSP1 (green) fully surrounds each daughter merozoite while PyBLEB is found only at the basal end. **b)** PyBLEB (magenta) localizes to puncta on the periphery of female gametocytes and **c)** male gametocytes. Single Z slices of merged channels. Scale bar = 1 μm.

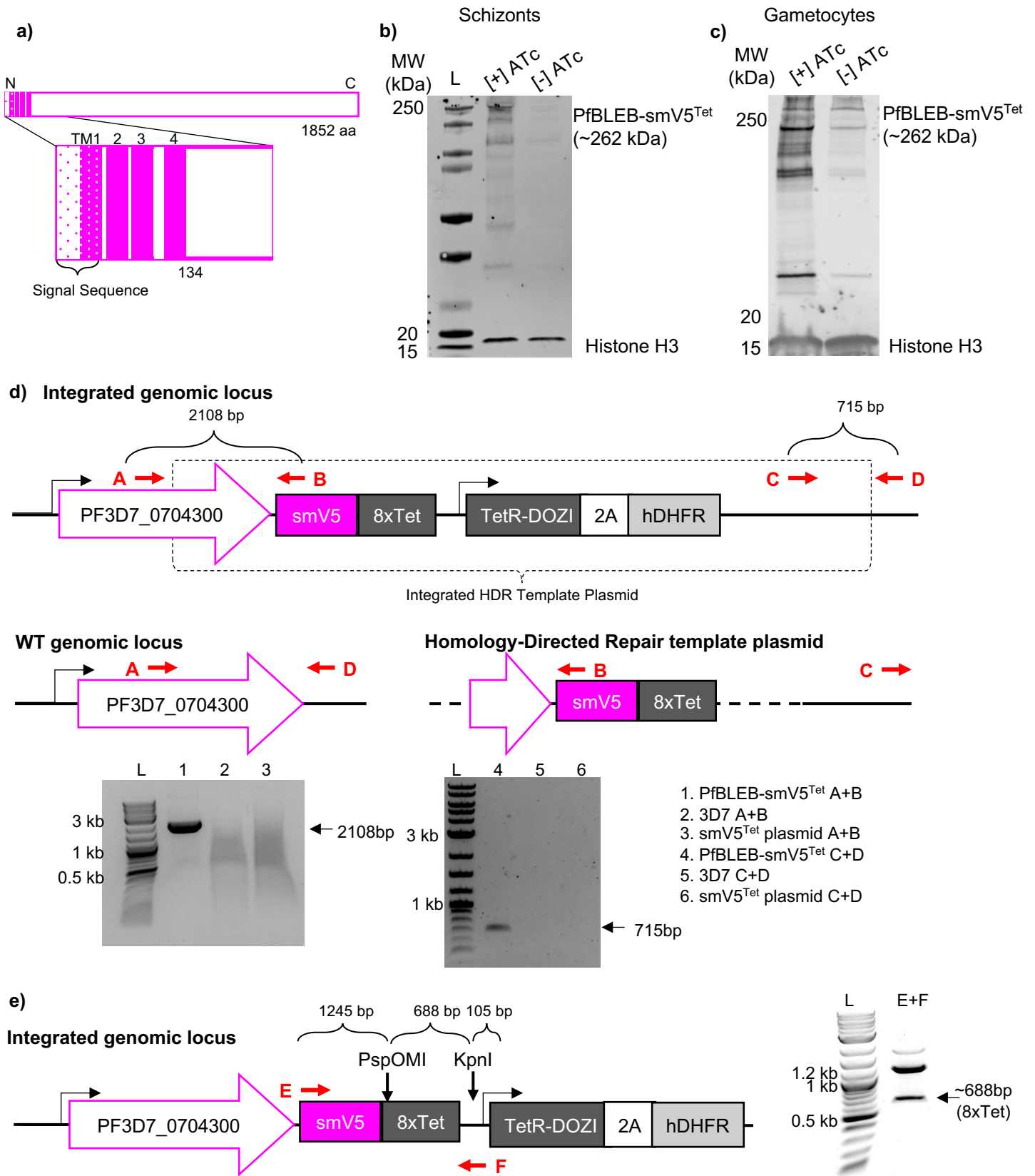


Fig. S5. Knockdown of PfBLEB via 8xTet/TetR-DOZI system. **a)** Predicted domains of PfBLEB protein. Coordinates of predicted transmembrane domains from PlasmoDB. PfBLEB has four predicted transmembrane (TM) domains clustered within the first 134 amino acids of the protein. **b-c)** Western blot with anti-V5 antibody reveals 87±14% (mean±SD, n=3) knockdown of PfBLEB-smV5^{Tet} in schizonts (**b**) and 65±18% (mean±SD, n=2) knockdown in gametocytes (**c**) upon removal of anhydrotetracycline (ATc). PfBLEB-smV5^{Tet} parasites were grown in the presence or

absence of ATc for two cycles. Quantification compared to histone H3 loading control. **d)** Integration PCR for PFBLEB-smV5^{Tet} with primers A and B or C and D compared to wildtype genomic DNA and homology-directed repair template plasmid. **e)** PCR confirmation of aptamer length. PCR with primers E and F, digested with PspOMI and KpnI restriction enzymes.

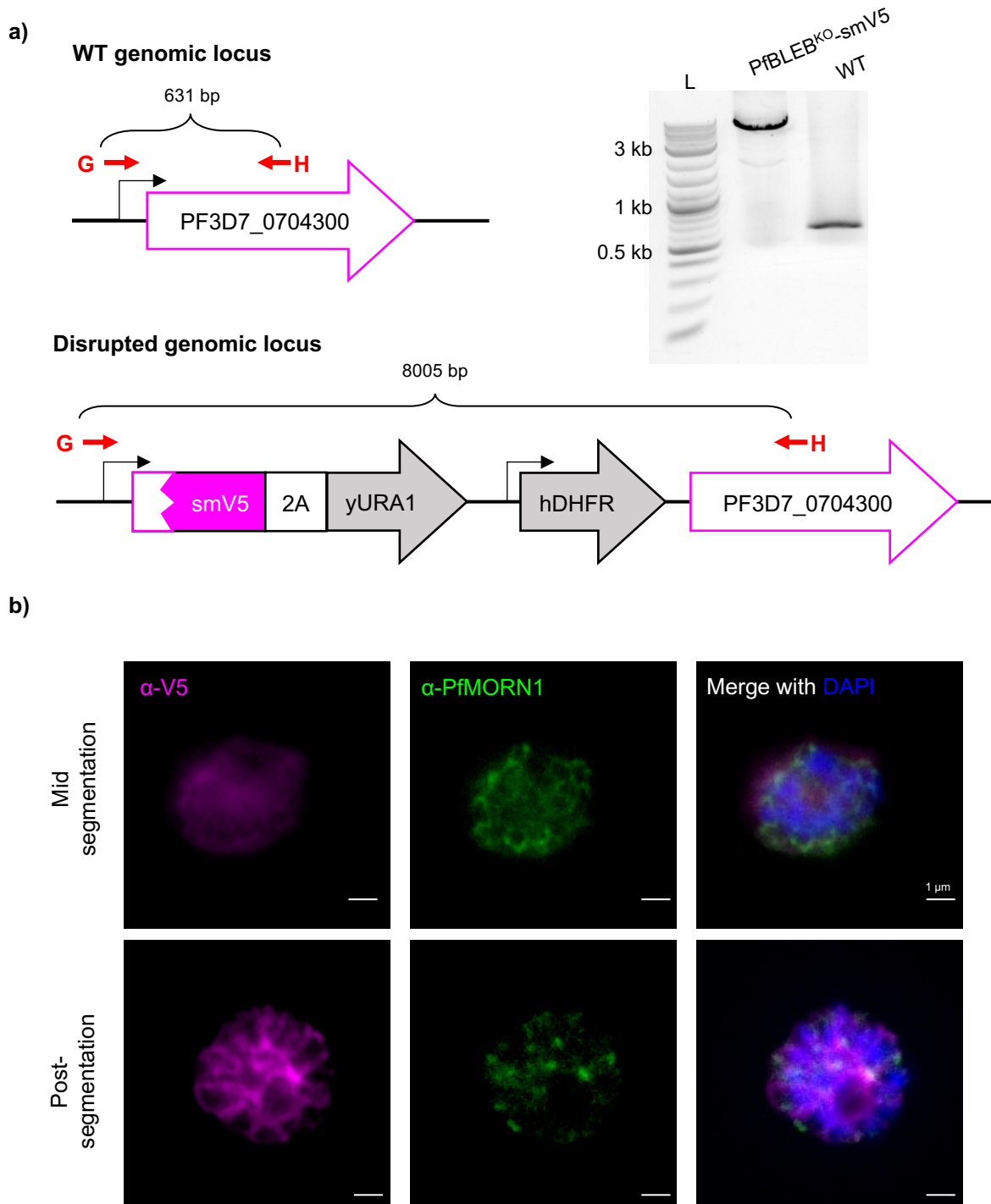


Fig. S6. PFBLEB is dispensible for asexual replication. a) Design and integration PCR of PFBLEB^{KO}. This disruption of the PFBLEB locus was constructed using an adapted SLI-TGD approach and confirmed via PCR amplification with Primer G and H. b) Immunofluorescence of in-frame smV5 epitope tag in PFBLEB^{KO} schizont stage parasites. PfMORN1 is a basal complex protein. Widefield microscopy with Olympus BX40 microscope and 100x oil objective. Scale bar = 1 μ m.

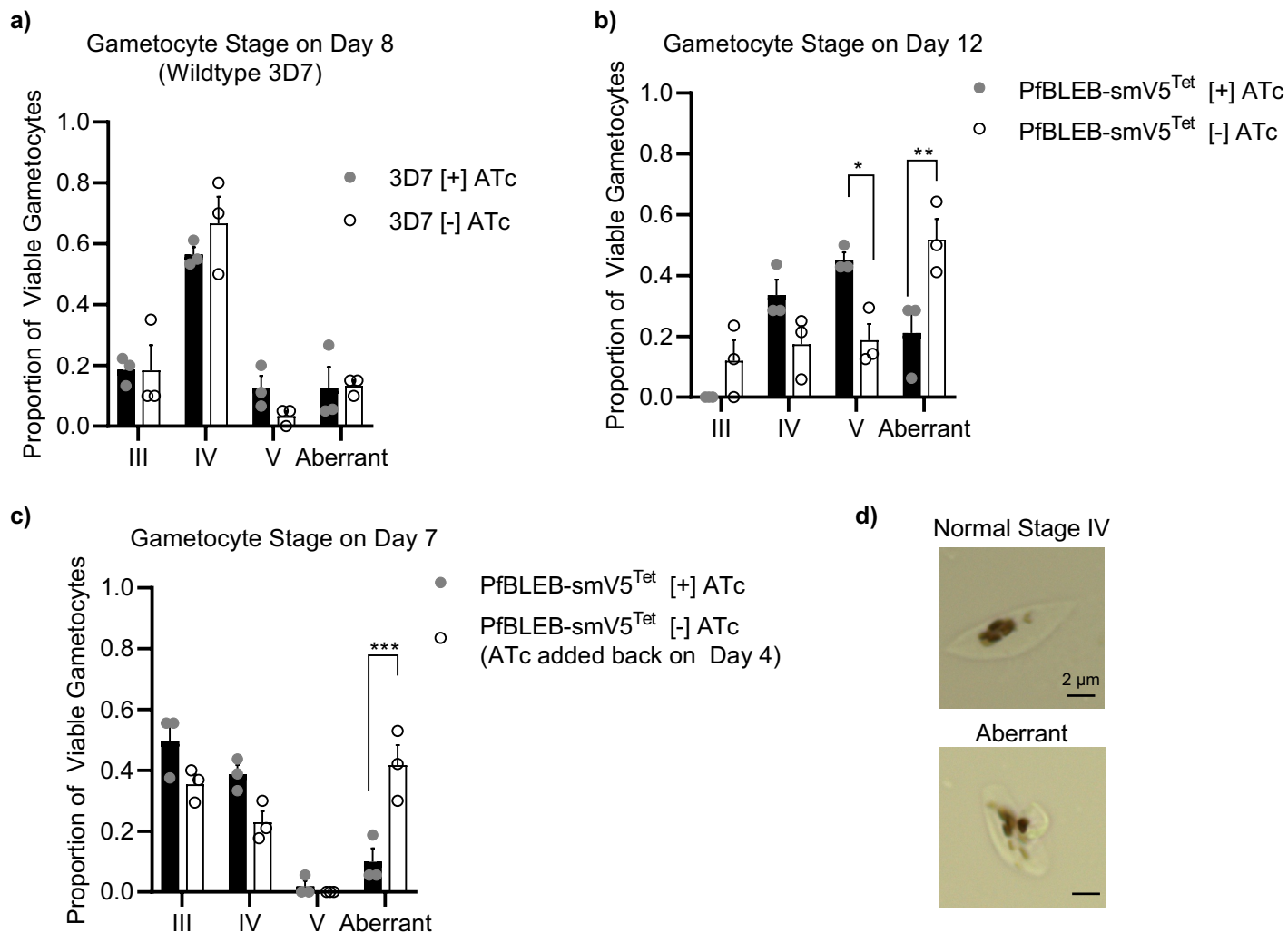


Fig. S7. Loss of PfBLEB disrupts gametocyte development. **a)** Wildtype parasites develop normally in the presence of ATc. Gametocyte formation was induced in wildtype 3D7 parasites in the presence or absence of ATc. Gametocyte stage was determined 8 days post-induction via Hemacolor stain. Two-way ANOVA. All timepoints not significantly different between presence and absence of ATc. Mean \pm standard error of the mean. N=3 technical replicates per experiment, representative of 3 independent experiments. **b)** Knockdown of PfBLEB results in a larger proportion of gametocytes with aberrant morphology and a smaller proportion of mature (stage IV-V) gametocytes. Gametocyte formation was induced in PfBLEB-smV5^{Tet} parasites in the presence or absence of ATc. Gametocyte stage was determined 12 days after gametocyte induction via Hemacolor stain. Two-way ANOVA. Mean \pm standard error of the mean. N=3. *: $p < 0.05$, **: $p < 0.01$. **c)** Parasites lacking PfBLEB during stages I-III are unable to recover when ATc is added back to the culture media during stage III. Gametocyte formation was induced in PfBLEB-smV5^{Tet} parasites in the presence or absence of ATc. In the PfBLEB-deficient condition, ATc was added back to the culture media 4 days post-induction. Gametocyte stage was determined 7 days after gametocyte induction via Hemacolor stain. Mean \pm standard error of the mean. N=3. **d)** Sample brightfield images of parasites from normal stage IV and aberrant categories. Scale bar = 2 μ m. ATc = anhydrotetracycline

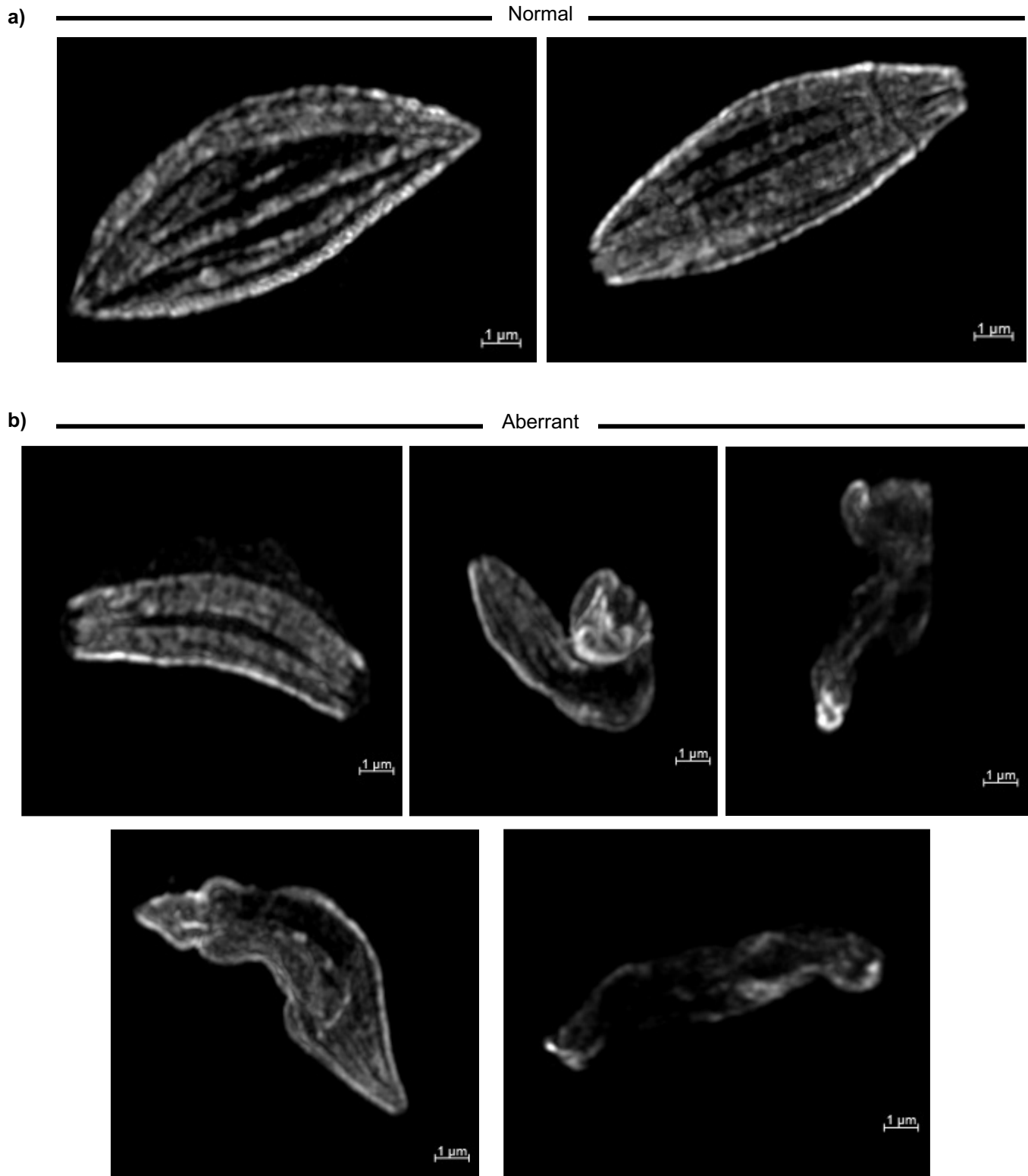
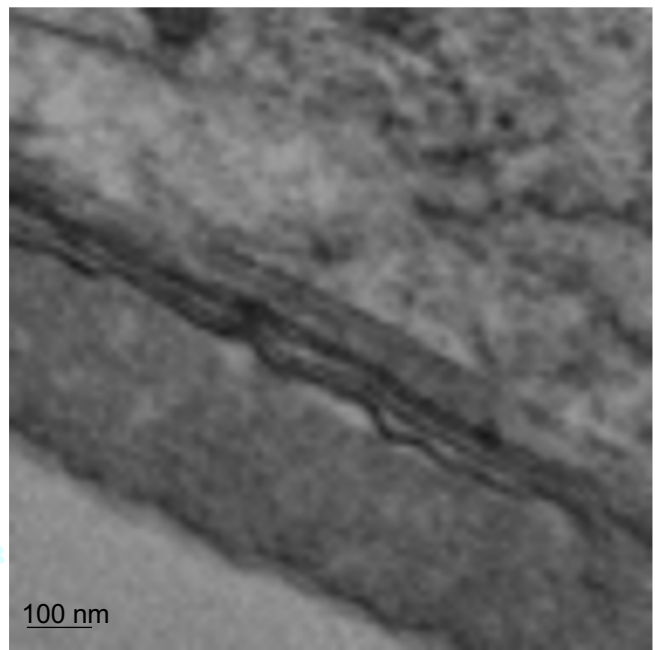
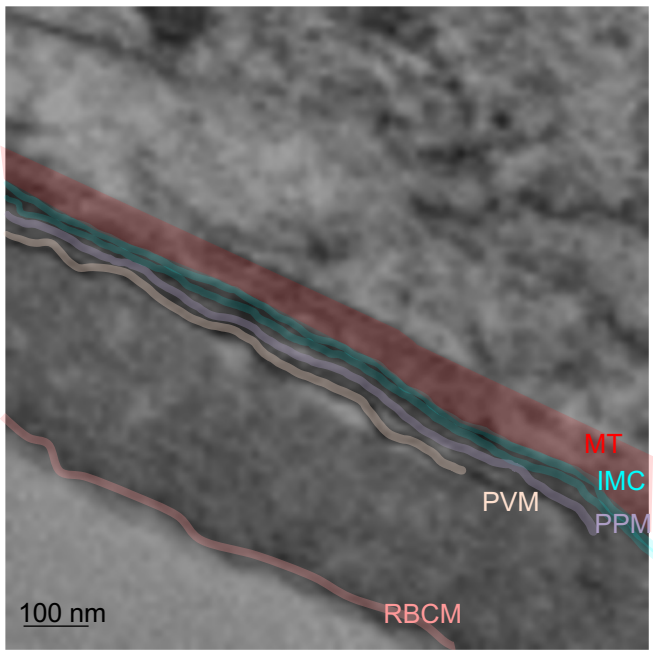


Fig. S8. Knockdown of PFBLEB disrupts the expansion of the inner membrane complex and microtubule network in gametocytes. Gametocyte formation was induced in PFBLEB-smV5^{Tet} parasites in the presence or absence of ATc. Immunofluorescence of α -tubulin on Day 10 after gametocyte induction demonstrates an incohesive microtubule network in PFBLEB knockdown parasites. Example images from “normal” (a) and “aberrant” (b) categories shown as maximum intensity projections of SR-SIM images. These are the same images as Fig. 4, shown here with only the α -tubulin channel for clarity. Scale bars = 1 μ m. ATc = anhydrotetracycline

a) [+]
ATc



b) [-]
ATc

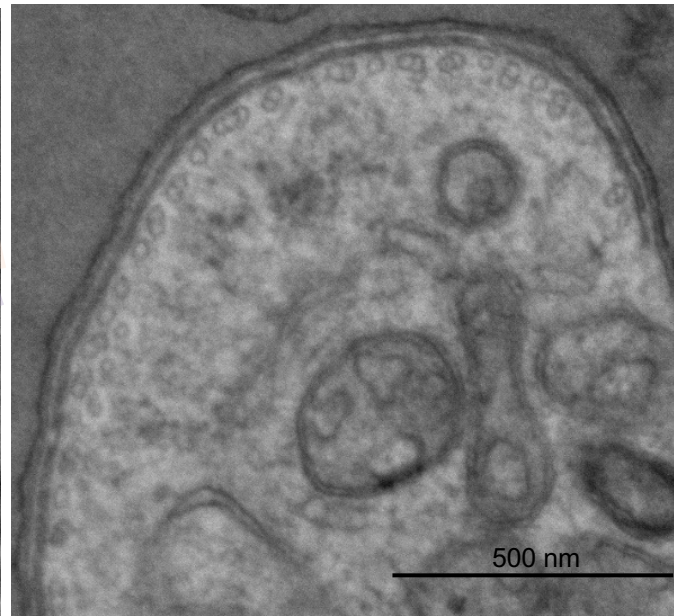
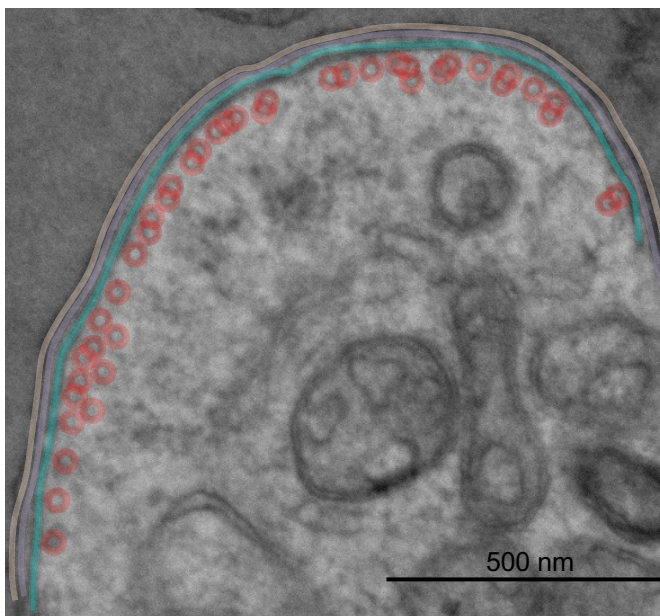


Fig. S9. Knockdown of PfBLEB disrupts the expansion of the inner membrane complex and microtubule network in gametocytes. This figure is the same as Figure 4, with pseudocoloring and labels removed. Transmission electron microscopy of gametocytes grown in the presence (a) or absence (b) of ATc on Day 8 after gametocyte induction. Color added on top of image to emphasize features (left) or removed (right). MT = subpellicular microtubules, red. IMC = inner membrane complex, cyan. PPM = parasite plasma membrane, purple. PVM = parasitophorous vacuolar membrane, tan. RBCM = red blood cell membrane, pink. Representative images of gametocytes in the “aberrant” category. ATc = anhydrotetracycline

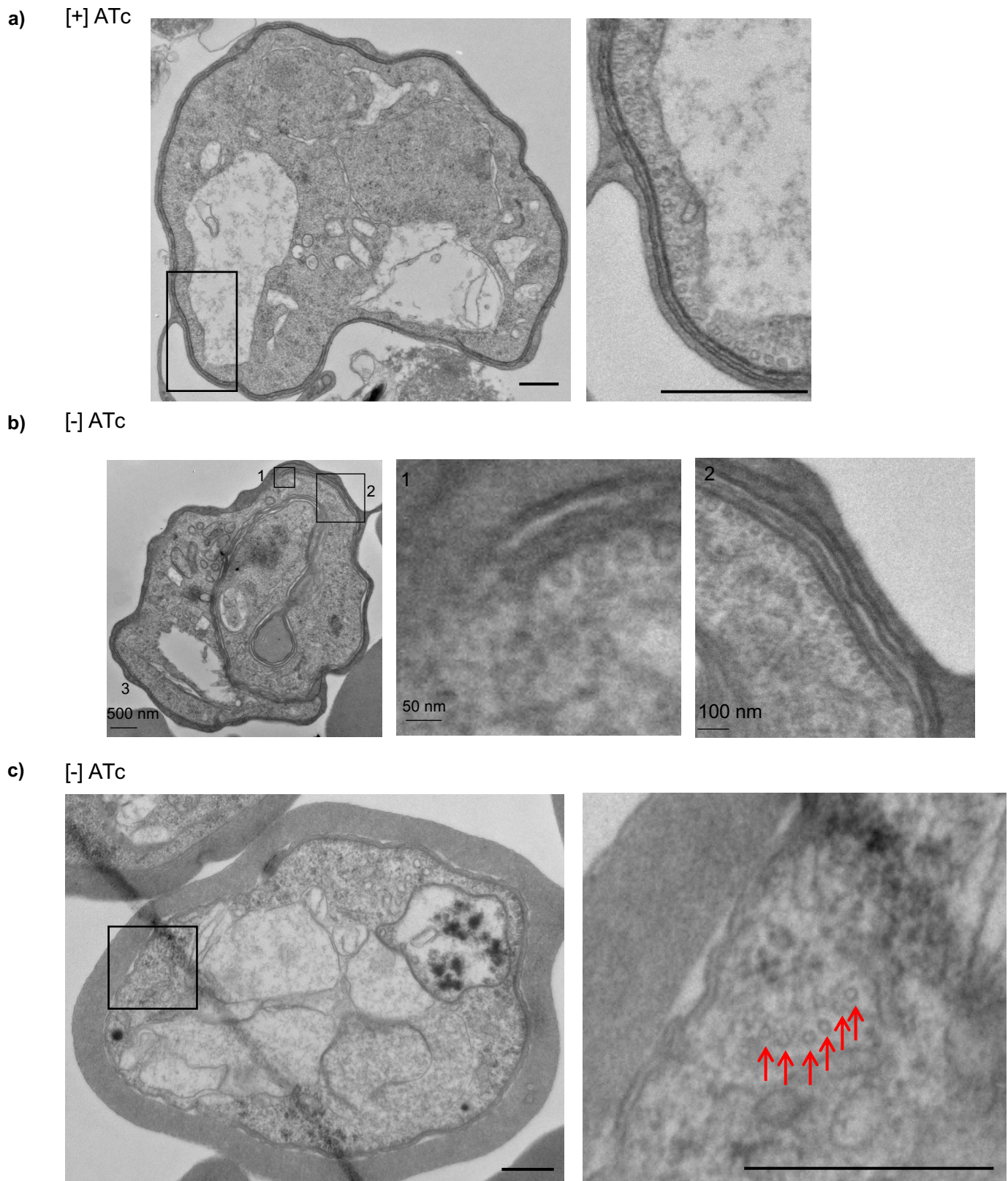


Fig. S10. Knockdown of PfBLEB disrupts the expansion of the inner membrane complex and microtubule network in gametocytes. Transmission electron microscopy of gametocytes grown in the presence (a) or absence (b) and (c) of ATc on Day 8 after gametocyte induction. In the presence of ATc, microtubules are evenly spaced in a single layer below the inner membrane complex (IMC). Scale bars = 500 nm. Representative images from each category. Left panels show full cell, right panels zoom in on areas of interest. ATc: anhydrotetracycline.

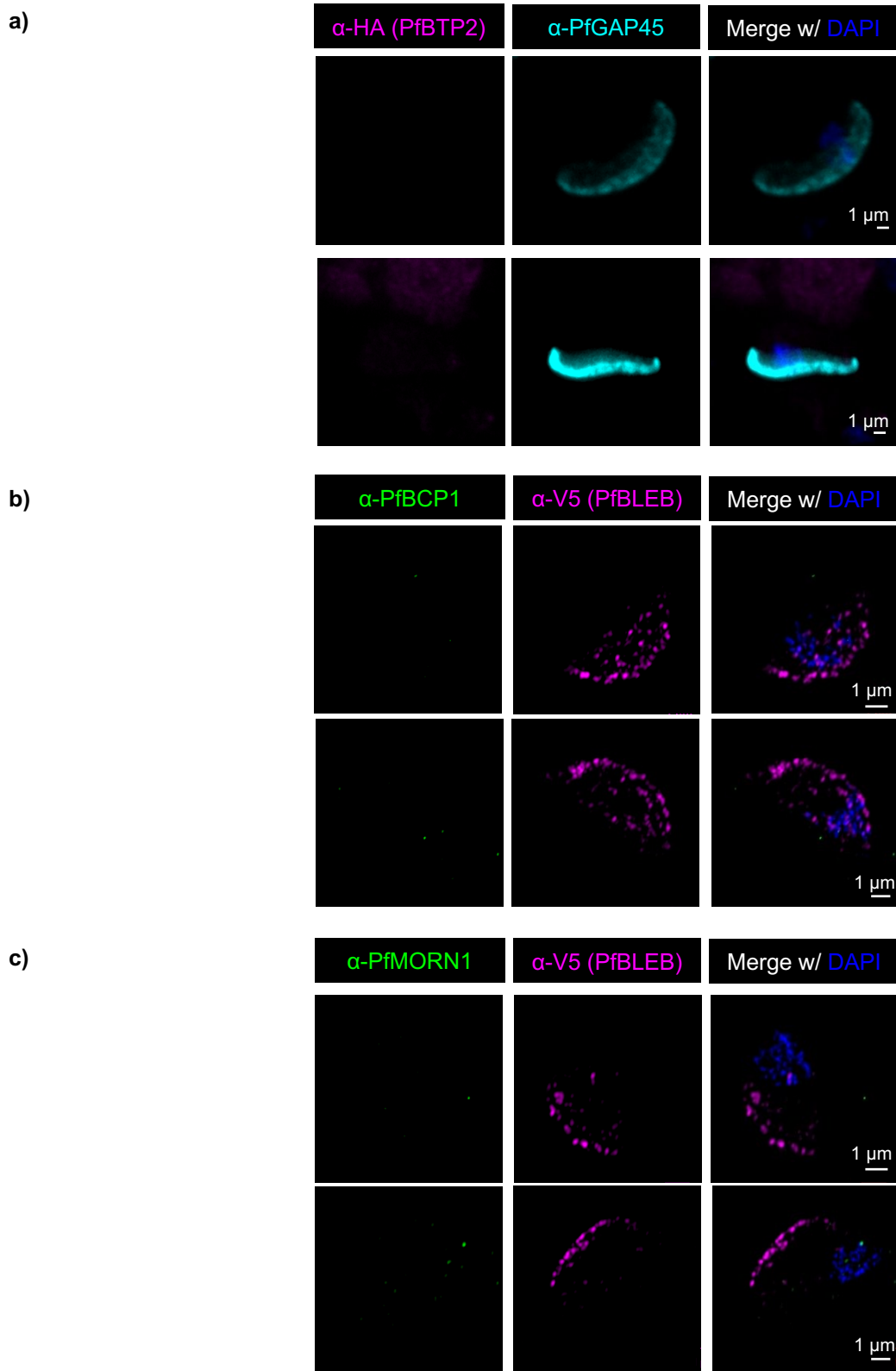


Fig. S11. Immunofluorescence of basal complex proteins in immature gametocytes. **a)** PfBTP2-3xHA (magenta) and PfGAP45 (cyan). Widefield microscopy with Olympus BX40 microscope and 100x oil objective. **b)** PfBCP1 (green) and PfBLEB-smV5 (magenta). Maximum intensity projection of SR-SIM images. **c)** PfMORN1 (green) and PfBLEB-smV5 (magenta). Maximum intensity projection of SR-SIM images. Scale bar = 1 μ m.

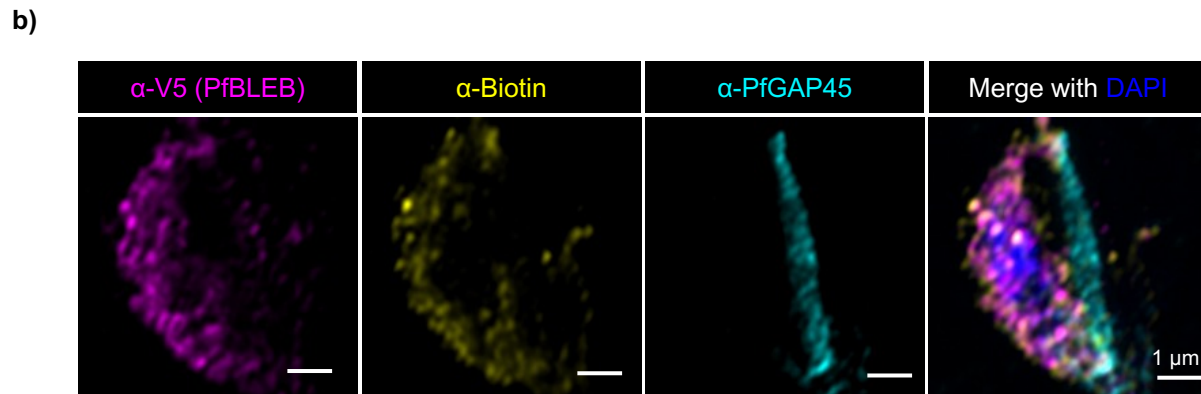
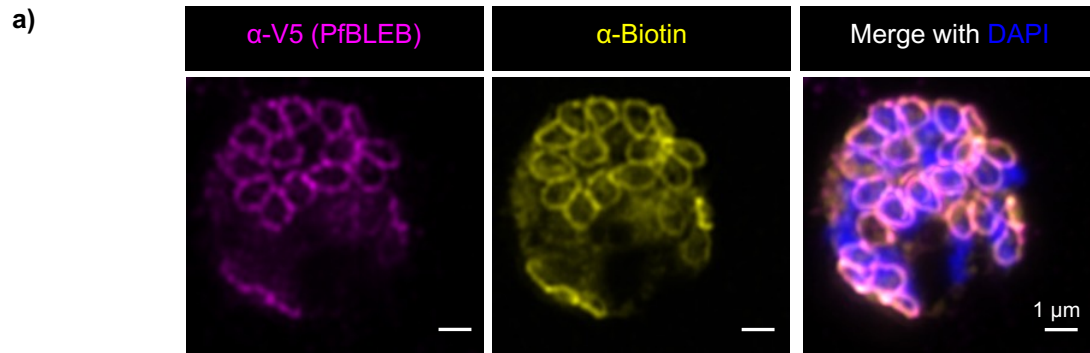


Fig. S12. Fusion of TurboID to PfBLEB does not alter its localization in schizonts or gametocytes.

Immunofluorescence demonstrates expected PfBLEB-V5-TurboID localization to **a)** the basal complex in segmenting schizonts or **b)** the area of plasma membrane devoid of inner membrane complex marker PfGAP45 (cyan) in gametocytes. Anti-biotin antibody (yellow) staining overlaps with V5 staining (magenta). Airyscan images shown are single z-slices for individual channels and maximum intensity projections of merged channels. Scale bars = 1 μ m.

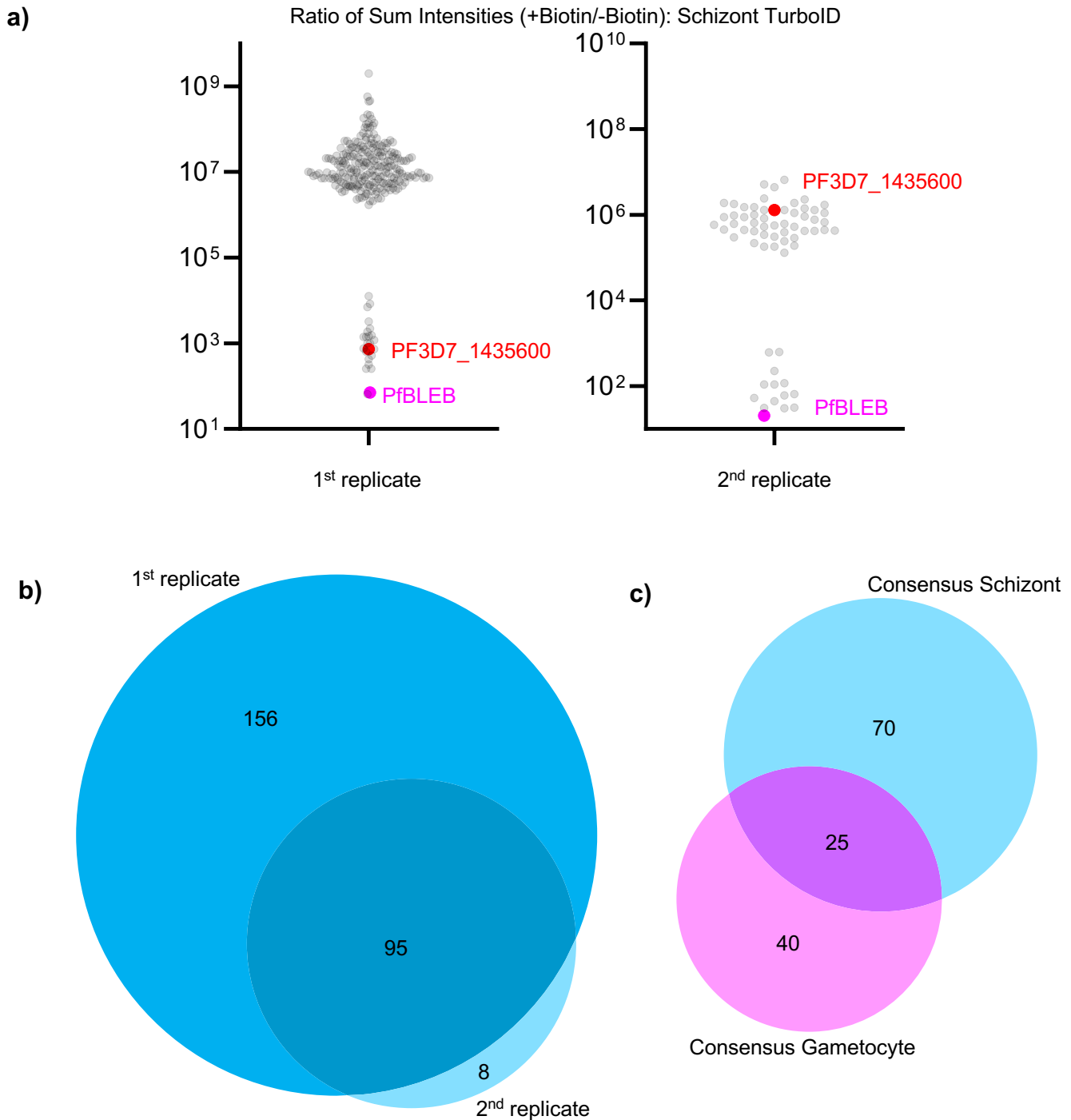


Fig. S13. Proximity-dependent biotinylation reveals proteins that reside near PfBLEB during schizogony. **a)** Dot plots showing the ratio of the sum intensity in the presence/absence of biotin of proteins detected via mass spectrometry of PfBLEB-TurboID schizonts. For proteins that were absent in the no biotin control, the sum intensity was arbitrarily set to 1 (to prevent dividing by zero). Thresholds were set to require more unique peptides than streptavidin. **b)** An area-proportional Venn diagram comparing the proteins identified in both schizont TurboID replicates. **c)** An area-proportional Venn diagram comparing the proteins identified in both schizont TurboID replicates and both gametocyte TurboID replicates.

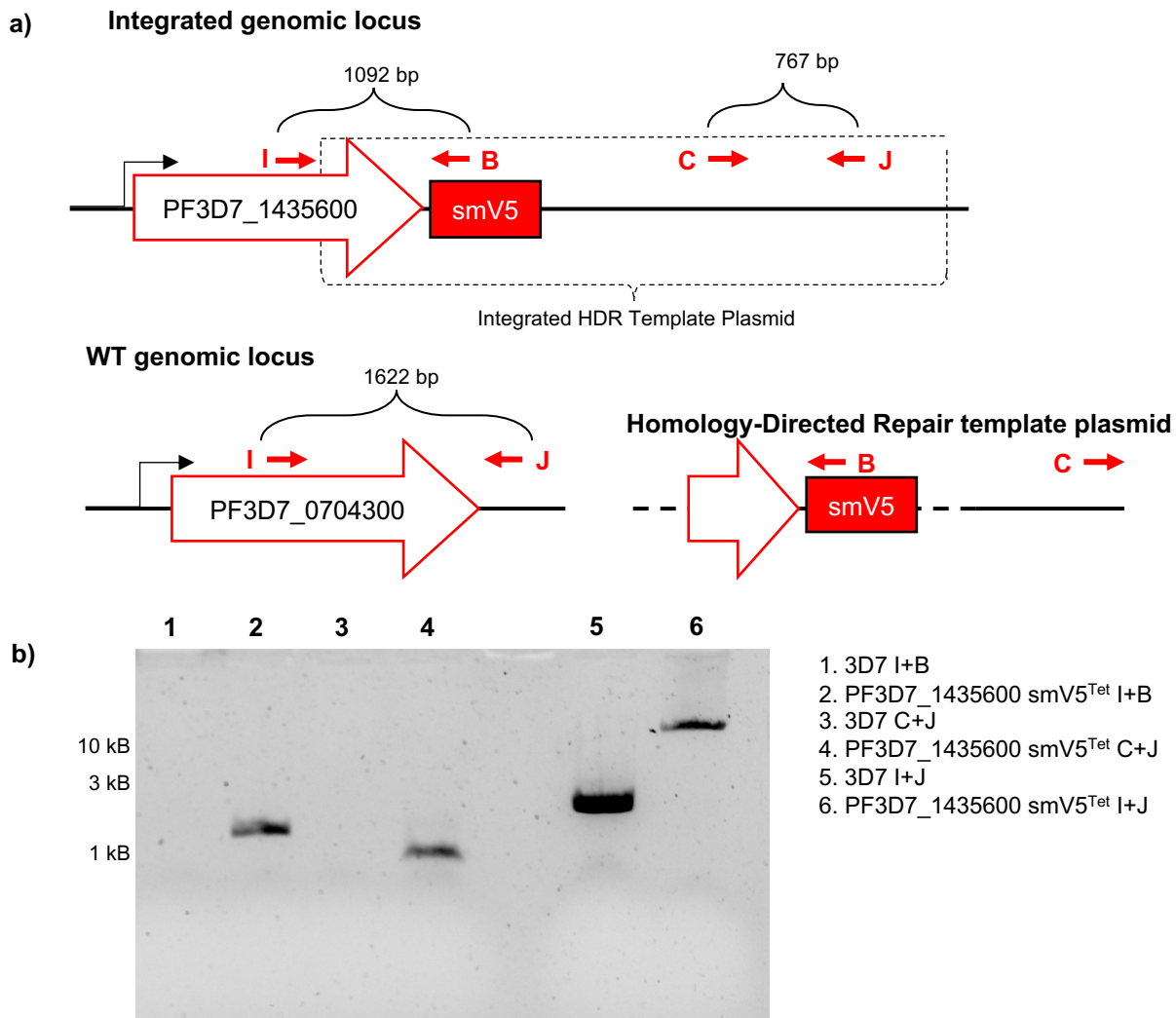


Fig. S14. Design and integration of PF3D7_1435600-smV5. **a)** Diagram depicting the expected genomic locus of PF3D7_1435600-smV5 parasites following integration of the homology directed repair template plasmid into the genomic locus, with the expected sizes for integration PCRs delineated. **b)** Integration PCRs for PF3D7_1435600-smV5.

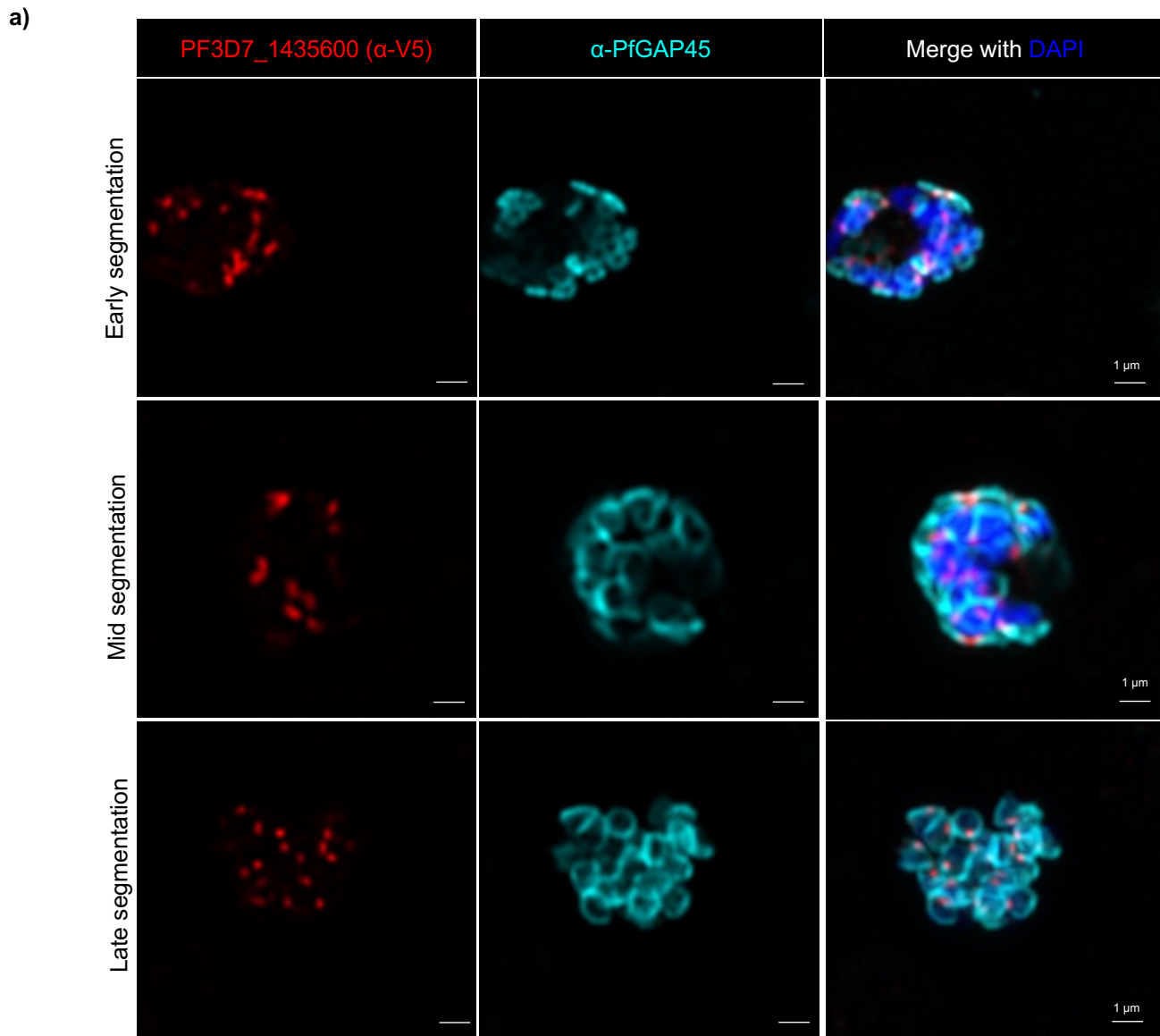


Fig. S15. PF3D7_1435600 localizes to distinct foci in schizonts. a) Immunofluorescence demonstrates that PF3D7_1435600-smV5 (red) localizes to distinct, punctate foci throughout schizogony, adjacent to the inner membrane complex-associated protein PfGAP45 (cyan). Airyscan images shown are single Z-slices for individual channels or maximum intensity projections of merged channels. Scale bars = 1 μ m.

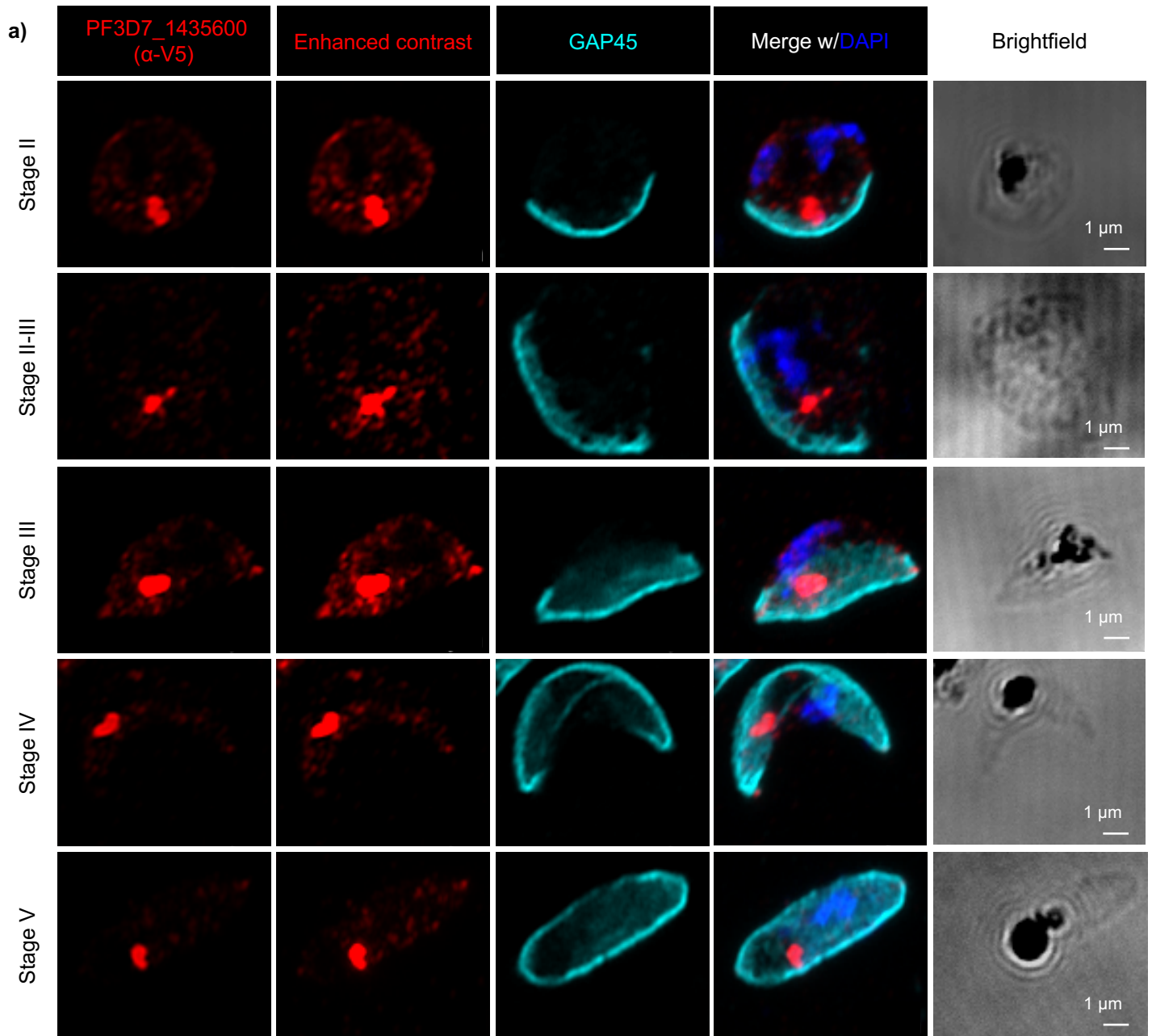


Fig. S16. PF3D7_1435600 localizes adjacent to the inner membrane complex in gametocytes. a)

Immunofluorescence demonstrates localization of PF3D7_1435600-smV5 (red) adjacent to the inner membrane complex-associated protein PfGAP45 (cyan) throughout gametocytogenesis. Airyscan images shown are single Z-slices for individual channels or maximum intensity projections of merged channels. Enhancing the contrast on images (second column) reveals faint staining in the same area as PfBLEB localization in addition to the bright, IMC-adjacent foci. Scale bars = 1 μ m.

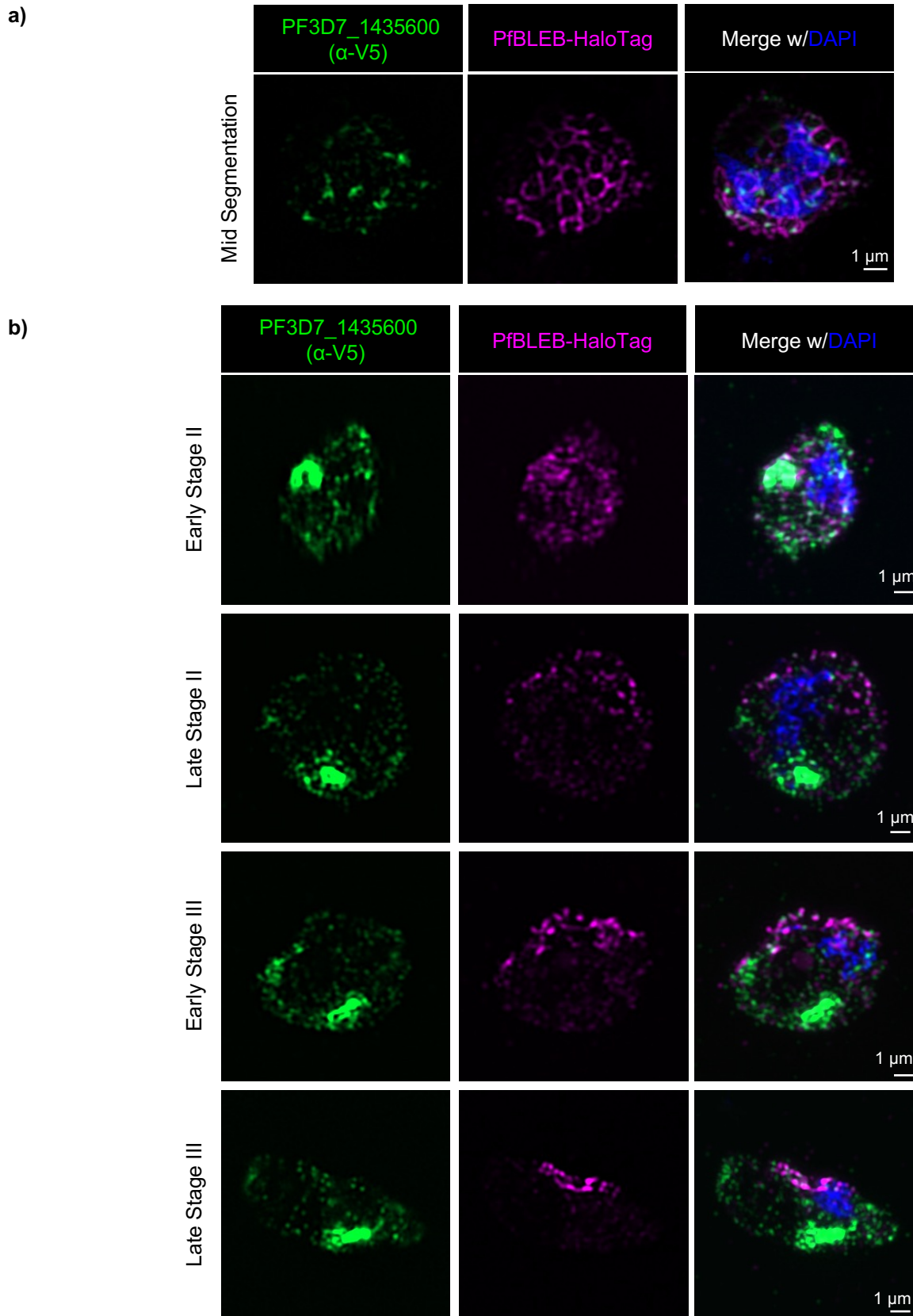


Fig. S17. PF3D7_1435600 and PfBLEB have distinct localization patterns in schizonts and gametocytes.

Immunofluorescence demonstrates localization of PF3D7_1435600-smV5 (green) and PfBLEB-HaloTag (magenta) (**a**) during schizogony or (**b**) throughout gametocytogenesis. Airyscan images shown are single Z-slices for individual channels or maximum intensity projections of merged channels. Scale bars = 1 μ m.

| Gene ID | Organism | Score | E-Value | Protein Length | Molecular Weight | Falciform gametocyte? |
|------------------|---|----------|-----------|----------------|------------------|-----------------------|
| PF3D7_0704300 | Plasmodium falciparum 3D7 | 3.55E+03 | 0.00E+00 | 1852 | 217493 | Yes |
| PADL01_0703000 | Plasmodium adleri G01 | 1211 | 0.00E+00 | 1696 | 199822 | No |
| PBANKA_0802000 | Plasmodium berghei ANKA | 288 | 3.00E-77 | 2046 | 236836 | No |
| PBILCG01_0703500 | Plasmodium billcollinsi G01 | 487 | 9.00E-141 | 1885 | 222653 | Yes |
| PBLACG01_0703400 | Plasmodium blacklocki G01 | 1671 | 0.00E+00 | 1877 | 221508 | No |
| PCHAS_0802300 | Plasmodium chabaudi chabaudi | 283 | 1.00E-75 | 1872 | 214602 | No |
| PCOAH_00000330 | Plasmodium coatneyi Hackeri | 312 | 9.00E-85 | 1862 | 208470 | No |
| PCYB_011170 | Plasmodium cynomolgi strain B | 312 | 1.00E-84 | 2003 | 225427 | No |
| PcyM_0104600 | Plasmodium cynomolgi strain M | 312 | 9.00E-85 | 2028 | 228213 | No |
| Pf7G8_070009700 | Plasmodium falciparum 7G8 | 2.56E+03 | 0.00E+00 | 1995 | 232042 | Yes |
| PfCD01_070008200 | Plasmodium falciparum CD01 | 3.08E+03 | 0.00E+00 | 1860 | 218233 | Yes |
| PfDd2_070008500 | Plasmodium falciparum Dd2 | 3.08E+03 | 0.00E+00 | 1881 | 220564 | Yes |
| PfGA01_070007700 | Plasmodium falciparum GA01 | 3.08E+03 | 0.00E+00 | 1875 | 219913 | Yes |
| PfGB4_070009500 | Plasmodium falciparum GB4 | 3.03E+03 | 0.00E+00 | 1840 | 216549 | Yes |
| PfGN01_070009400 | Plasmodium falciparum GN01 | 3.06E+03 | 0.00E+00 | 1878 | 220408 | Yes |
| PfHB3_070008300 | Plasmodium falciparum HB3 | 3.06E+03 | 0.00E+00 | 1899 | 222304 | Yes |
| PfIT_070009200 | Plasmodium falciparum IT | 3.08E+03 | 0.00E+00 | 1895 | 221744 | Yes |
| PfKE01_070007900 | Plasmodium falciparum KE01 | 3.06E+03 | 0.00E+00 | 1900 | 223039 | Yes |
| PfKH01_070008300 | Plasmodium falciparum KH01 | 3.07E+03 | 0.00E+00 | 1883 | 220806 | Yes |
| PfKH02_070007600 | Plasmodium falciparum KH02 | 3.07E+03 | 0.00E+00 | 1875 | 220007 | Yes |
| PfML01_070008700 | Plasmodium falciparum ML01 | 3.09E+03 | 0.00E+00 | 1870 | 219193 | Yes |
| PfML01_130041400 | Plasmodium falciparum ML01 | 4.43E+01 | 5.00E-03 | 2952 | 348712 | Yes |
| PfSD01_070008200 | Plasmodium falciparum SD01 | 3.08E+03 | 0.00E+00 | 1893 | 221556 | Yes |
| PfSN01_070009100 | Plasmodium falciparum SN01 | 2.99E+03 | 0.00E+00 | 1807 | 212679 | Yes |
| PfTG01_070009300 | Plasmodium falciparum TG01 | 3.00E+03 | 0.00E+00 | 1805 | 212518 | Yes |
| AK88_00965 | Plasmodium fragile strain nilgiri | 298 | 2.00E-80 | 1917 | 215401 | No |
| PGABG01_0702900 | Plasmodium gaboni strain G01 | 648 | 0.00E+00 | 1710 | 201947 | Yes |
| PGSY75_0704300 | Plasmodium gaboni strain SY75 | 1096 | 0.00E+00 | 1630 | 192979 | Yes |
| PGAL8A_00044400 | Plasmodium gallinaceum 8A | 224 | 1.00E-57 | 2285 | 269780 | No |
| C922_03020 | Plasmodium inui San Antonio 1 | 44.3 | 8.00E-03 | 1968 | 220830 | No |
| PmUG01_01015800 | Plasmodium malariae UG01 | 315 | 2.00E-85 | 2681 | 313170 | No |
| PocGH01_01012100 | Plasmodium ovale curtisi GH01 | 313 | 8.00E-85 | 2070 | 237126 | No |
| PPRFG01_0703800 | Plasmodium praefalciparum strain G01 | 3009 | 0.00E+00 | 1863 | 219083 | No |
| PRCDC_0702500 | Plasmodium reichenowi CDC | 2692 | 0.00E+00 | 1920 | 225652 | Yes |
| PRG01_0702500 | Plasmodium reichenowi G01 | 1063 | 0.00E+00 | 1914 | 225398 | Yes |
| PRELSG_0101800 | Plasmodium relictum SGS1-like | 280 | 9.00E-75 | 1791 | 212207 | No |
| YYG_01121 | Plasmodium vinckei petteri strain CR | 286 | 9.00E-77 | 1912 | 220424 | No |
| YYE_01819 | Plasmodium vinckei vinckei strain vinckei | 278 | 3.00E-74 | 1914 | 220237 | No |
| PVP01_0104500 | Plasmodium vivax P01 | 325 | 1.00E-88 | 1970 | 219854 | No |
| PVX_087755 | Plasmodium vivax Sal-1 | 325 | 1.00E-88 | 2004 | 223577 | No |
| PVL_010007200 | Plasmodium vivax-like Pvl01 | 47 | 1.00E-03 | 1208 | 134876 | No |
| PY17X_0804700 | Plasmodium yoelii yoelii 17X | 265 | 3.00E-70 | 2095 | 241539 | No |
| PY01947 | Plasmodium yoelii yoelii 17XNL | 265 | 3.00E-70 | 2095 | 241539 | No |
| PYYM_0804600 | Plasmodium yoelii yoelii YM | 265 | 3.00E-70 | 2095 | 241539 | No |

Table S1. BLAST results for BLEB orthologs.

3D7-PfBLEB-TurboID in schizonts

(top 20 hits by number of unique peptides in run 1)

| GeneID | Annotation | Unique +Biotin Run 1 | Unique -Biotin Run 1 | Unique +Biotin Run 2 | Unique -Biotin Run 2 |
|---------------|---|-------------------------|-------------------------|-------------------------|-------------------------|
| PF3D7_0704300 | PfBLEB | 88 | 44 | 104 | 56 |
| PF3D7_0704100 | basal complex transmembrane protein 2 | 81 | 0 | 43 | 2 |
| PF3D7_0704600 | HECT-type E3 ubiquitin ligase UT | 76 | 0 | 9 | 0 |
| PF3D7_0407800 | protein CINCH | 75 | 7 | 41 | 2 |
| PF3D7_1018200 | serine/threonine protein phosphatase 8, putative | 65 | 0 | 23 | 0 |
| PF3D7_1229800 | myosin J, putative | 49 | 0 | 19 | 0 |
| PF3D7_1329100 | myosin F, putative | 46 | 1 | 19 | 2 |
| PF3D7_0915400 | ATP-dependent 6-phosphofructokinase | 43 | 2 | 26 | 2 |
| PF3D7_0929400 | high molecular weight rhoptry protein 2 | 42 | 0 | 3 | 0 |
| PF3D7_1142100 | conserved Plasmodium protein, unknown function | 42 | 0 | 26 | 0 |
| PF3D7_1308200 | carbamoyl phosphate synthetase | 39 | 2 | 17 | 0 |
| PF3D7_1435600 | conserved Plasmodium protein, unknown function | 38 | 4 | 18 | 0 |
| PF3D7_0703500 | erythrocyte membrane-associated antigen | 39 | 0 | 14 | 0 |
| PF3D7_1436200 | basal complex protein BCP1 | 37 | 0 | 5 | 0 |
| PF3D7_0524000 | karyopherin beta | 35 | 0 | 29 | 7 |
| PF3D7_0510100 | KH domain-containing protein, putative | 35 | 0 | 10 | 0 |
| PF3D7_1252100 | rhoptry neck protein 3 | 35 | 0 | 0 | 0 |
| PF3D7_1419400 | conserved Plasmodium membrane protein, unknown function | 32 | 0 | 19 | 0 |
| PF3D7_1312900 | eukaryotic translation initiation factor 4 gamma | 31 | 0 | 21 | 1 |
| PF3D7_1219000 | formin 2 | 30 | 0 | 10 | 0 |

NF54-PfBLEB-TurboID in stage II-III gametocytes

(top 20 hits by number of unique peptides in run 1)

| | | | | | |
|---------------|---|----|----|-----|----|
| PF3D7_0704300 | PfBLEB | 88 | 0 | 127 | 61 |
| PF3D7_1435600 | conserved Plasmodium protein, unknown function | 42 | 0 | 82 | 13 |
| PF3D7_1327300 | conserved Plasmodium protein, unknown function | 35 | 17 | 55 | 23 |
| PF3D7_1219100 | clathrin heavy chain, putative | 31 | 0 | 80 | 27 |
| PF3D7_0818900 | heat shock protein 70 | 27 | 4 | 26 | 19 |
| PF3D7_0606600 | conserved Plasmodium protein, unknown function | 27 | 0 | 53 | 4 |
| PF3D7_1103800 | CCR4-NOT transcription complex subunit 1, putative | 26 | 0 | 69 | 2 |
| PF3D7_1466800 | NOC3 domain-containing protein, putative | 23 | 0 | 38 | 8 |
| PF3D7_0523000 | multidrug resistance protein 1 | 23 | 0 | 44 | 24 |
| PF3D7_0314700 | RING finger protein RNF1 | 23 | 0 | 43 | 10 |
| PF3D7_0927200 | zinc finger protein, putative | 20 | 0 | 38 | 5 |
| PF3D7_0703500 | erythrocyte membrane-associated antigen | 20 | 0 | 57 | 11 |
| PF3D7_1142100 | conserved Plasmodium protein, unknown function | 19 | 0 | 93 | 9 |
| PF3D7_0215000 | acyl-CoA synthetase | 15 | 13 | 6 | 1 |
| PF3D7_1219000 | formin 2 | 18 | 0 | 95 | 2 |
| PF3D7_0708400 | heat shock protein 90 | 16 | 1 | 38 | 31 |
| PF3D7_1355600 | PhIL1 interacting protein PIP1 | 15 | 5 | 24 | 3 |
| PF3D7_1107300 | polyadenylate-binding protein-interacting protein 1 | 15 | 0 | 40 | 6 |
| PF3D7_1357000 | elongation factor 1-alpha | 15 | 2 | 25 | 22 |
| PF3D7_1329100 | myosin F, putative | 15 | 0 | 83 | 21 |

Table S2. TurboID hits.

| Name | Sequence |
|--------------|--|
| oJDD1525 (A) | 5'-TGTGCGGCCGCAATAATAGTACTACACAAAAGAAAGTACCTTC-3' |
| oJDD2933 (B) | 5'-CTGCTGCTGAGTACTATCAAGTC-3' |
| oJDD56 (C) | 5'-ACACTTTATGCTCCGGCTCGTATGTTGTG-3' |
| oJDD6010 (D) | 5'-GATAGGATAAGTTTTTGAATATTTTATTATTGTTAC-3' |
| oJDD2239 (E) | 5'-TAGGGATCCCCCGGATGGGAAAACCTATACCGAACCCCTCCTTGGA-3' |
| oJDD44 (F) | 5'-TGGGGTGATGATAAAATGAAAG-3' |
| oJDD4756 (G) | 5'-ACATTTAGATACTTACTCTC-3' |
| oJDD4489 (H) | 5'-CTTTATTACATGTGTTTAGCTGATTC-3' |
| oJDD6917 (I) | 5' -GAACTACTAGTAAACAGAATACAACAACAGAG- 3' |
| oJDD6918 (J) | 5' -GGATAATAAACATGGTTAAAAGTATCTCAATATCTAGATATGG- 3' |
| oJDD4162 | 5'- AGGTATATTGTAAATATATGTATATATCTATGATATCAGGCCTCCTTTTGAACAAGATATAAATGAGG-3' |
| oJDD4165 | 5'-CTCCACTTCGTTGTTTCAGTACGGGGTATGTATATCTGTTTTGTGAACCTTGGCAGAATC-3' |
| oJDD4161 | 5'-CGCCGCGCGCCGCATGAAAAATGTATCGTTAAAGGGTATCTTAAG-3' |
| oJDD4163 | 5'-CCTCATTATATCTTGTTCAAAAGGAGGCCTGATATCATAGATATATACATATATTTACAATATACCT-3' |
| oJDD4401 | 5'-GCGGCGCCATGGTTTCTTTTTGTTCTTCTTGC GG-3' |
| oJDD4564 | 5'-TATCTGCAGGGATTTCTACACATCTTGAGGTTT-3' |
| oJDD4571 | 5'-TATAATATTGATGTTAGGAAAATCACAAGTGTTTTAGAGCTAGAAATAGCAAGTTAA-3' |
| oJDD4572 | 5'-GCTCTAAAACACTTGTGATTTTCTAACATCAATATTATATACTTAATATGAAATATG-3' |
| oJDD3059 | 5'-GTAAGGAGAAAATACCGCATCAGGCGCCAGCCTAGGTTTATGGTAGCCTTAAAACTTCA-3' |
| oJDD3273 | 5'-CTAACGCGTGCTAGAGGTGCTGCTGCTGGTCTGGAGGTGCAGGTAGAATGGGAAAACCTATACCGAAC-3' |
| oJDD4546 | 5'-CATTGGTCCTGGATTTTCTTCTACATCTCCAC-3' |
| oJDD4547 | 5'-GTGGAGATGTAGAAGAAAATCCAGGACCAATGACAGCCAGTTTAACTACCAAGTTCTTG-3' |
| oJDD4548 | 5'-TAGCTCGAGTTAAATGCTGTTCAACTCCCACGGAAC-3' |
| oJDD4159 | 5'-CGCCGCGCGCCGCTAGGAAAAGAATAAATACGATATAGA-3' |
| oJDD4160 | 5'-GCGGCGACGCGTTTTTTTTGTCCTTTTCTCATTGTATTA-3' |
| oJDD6573 | 5'-CGGCTTGTGACGACGCGGCTCTCCGTCGTGAGGATCATCGCGGCCGCAAGCTTTTACATATAATAAG-3' |
| oJDD6574 | 5'-GATGTTGACGAGTTGTCTTCATGCGGCTTGTGATGTGGAGCTTATTACCTTTACAACATCAAACATTTTC-3' |
| oJDD6575 | 5'-GAAATGTTTGTGTTGTAAGGTAATAAGCTCCACATCAACAAGCCGCATGAAGACAACCTCGTCGAACATC-3' |
| oJDD6576 | 5'-CAAGTCCAAGGAGGGGTTCCGGTATAGTTTTCCCATCCATGGCTTGTCTATAATCTTCTTCTGAGCGAC-3' |
| oJDD6453 | 5'-TATTGTAATATTTATACACAAACGA-3' |
| oJDD6454 | 5'-AAACTCGTTTGTGTATAAATATTAC-3' |
| oJDD6577 | 5'-TATTGTTAGATGAATTATCCTCGTG-3' |
| oJDD6578 | 5'-AAACCACGAGGATAATTCATCTAAC-3' |
| oJDD6579 | 5'-TATTGACATATAAATAAACCACAG-3' |
| oJDD6580 | 5'-AAACCGTGTGGTTTATTATATGTC-3' |
| oSL28-59 | 5'-GCGGTACCCGTTCAAAAAGTTCAAAAATCGATGAAAATGAACATTGAAAATTGCAG-3' |
| oSL28-60 | 5'-GATCACC GGTCGTCGACGATCTAGAACGATGAAATACCTGCGTTGTAATAATTACGATCGAGT-3' |
| oSL28-63 | 5'-CATCGTTCTAGATCGTCGACGAACCGGTGATCGCAAAAAGTAGCGAAATAAATGACATCAAAAACCTATG-3' |
| oSL28-64 | 5'-GCACTAGTATTTTTATTTTTTCGTTTTTTTTTTTTATTTTTATTGTTTTTATAATTTTTTGTGTTTGTATGC-3' |

Table S3. Oligo sequences for cloning and integration PCR.